Journal of Natural Gas Science and Engineering 26 (2015) 1607–1619

Contents lists available at ScienceDirect

Journal of Natural Gas Science and Engineering

journal homepage: www.elsevier.com/locate/jngse

Geomechanics of CO_2 enhanced shale gas recovery

Xiang Li*, Derek Elsworth

John and Willie Leone Family Department of Energy and Mineral Engineering, EMS Energy Institute and G³ Center, Pennsylvania State University, University Park, PA 16802, USA

ARTICLE INFO

Article history:
Received 14 July 2014
Accepted 11 August 2014
Available online 7 September 2014

Keywords:
CO_2-ESGR
Continuous injection
Pulsed injection
Permeability
CO_2 early breakthrough
CO_2 sequestration
Induced seismicity net neutrality

ABSTRACT

Shale gas has become an increasingly important source of natural gas (CH_4) in the United States over the last decade. Due to its unconventional characteristics, injecting carbondioxide (CO_2) to enhance shale gas recovery (ESGR) is a potentially feasible method to increase gas-yield while both affording a sink for CO_2 and in reducing the potential for induced seismicity. However, understanding of this issue is limited with few pilot field studies proposed. This study examines CO_2-ESGR to better understand its feasibility and effectiveness. We explore the roles of important coupled phenomena activated during gas substitution especially vigorous feedbacks between sorptive behavior and permeability evolution. Permeability and porosity evolution models developed for sorptive fractured coal are adapted to the component characteristics of gas shales. These adapted models are used to probe the optimization of CO_2-ESGR for injection of CO_2 at overpressures of 0 MPa, 4 MPa and 8 MPa to investigate magnitudes of elevated CH_4 production, CO_2 storage rate and capacity, and of CO_2 early-breakthrough and permeability evolution in the reservoir. For the injection pressures selected, CH_4 production was enhanced by 2.3%, 14.3%, 28.5%, respectively, over the case where CO_2 is not injected. Distinctly different evolutions are noted for permeability in both fractures and matrix due to different dominating mechanisms. Fracture permeability increased by ~1/3 for the injection scenarios due to the dominant influence of CH_4 de-sorption over CO_2 sorption. CO_2 sequestration capacity was only of the order of 10^4 m^3 when supercritical for a net recovery of CH_4 of 10^8 m^3. We investigated the potential of optimal CO_2-pulsed injection to enhance CH_4 production (absolute mass recovered)-without the undesirable effects of CO_2 early-breakthrough and also minimum cost on CO_2 injection. This utilizes the competitive sorptive behavior between CH_4 and CO_2, can also reduce the potential for induced seismicity hence the entire system can be near net neutrality in terms of its carbon and seismic footprint.

1. Introduction

Shale gas is providing the United States with a locally produced and secure source of natural gas that both improves energy security and has provided a renaissance in manufacturing. It has become an important source of natural gas in the US in the last decade. Annual natural-gas production from shale-gas is ~1.0 Tscf coming from more than 40,000 shale gas wells completed in 5 primary basins (Jenkins et al., 2008). However, shale gas extraction has experienced a variety of technical difficulties due to its unconventional attributes. Numerical simulation is a powerful tool that can integrate core, log, and well testing data to describe and quantify reservoir behavior by evaluating the effects of variations in key parameters. Such models can incorporate unique components such as anisotropy and heterogeneity as well as the contributions of free gas and sorbed gas, and be used to evaluate the effects of various development strategies including well spacing, well pattern, hydraulic fracturing design and water/gas flooding rate/schedule. Once the model is constructed, it can be updated with production data, reservoir pressures, and production bottomhole pressures obtained on a regular basis to better understand and predict future reservoir performance (Jenkins et al., 2008). Over the past decade, improved practices of reservoir stimulation and production have made gas shale a viable energy resource. Enhancing gas recovery through the injection of carbondioxide (CO_2) however is yet to be tested in the field (Hussen et al., 2012). Hence, further understanding the behavior of gas shale reservoirs and of methods to enhance its recovery remains important.

It is apparent that gas shale has the capacity to permanently store a considerable amount of gas. This is trapped both in adsorbed state within finely dispersed organic matter (i.e., kerogen) and also in free state within a nanoporous substrate comprising micropores

* Corresponding author. Tel.: +1 814 441 1206.
E-mail address: xzl111@psu.edu (X. Li).

http://dx.doi.org/10.1016/j.jngse.2014.08.010
1875-5100/

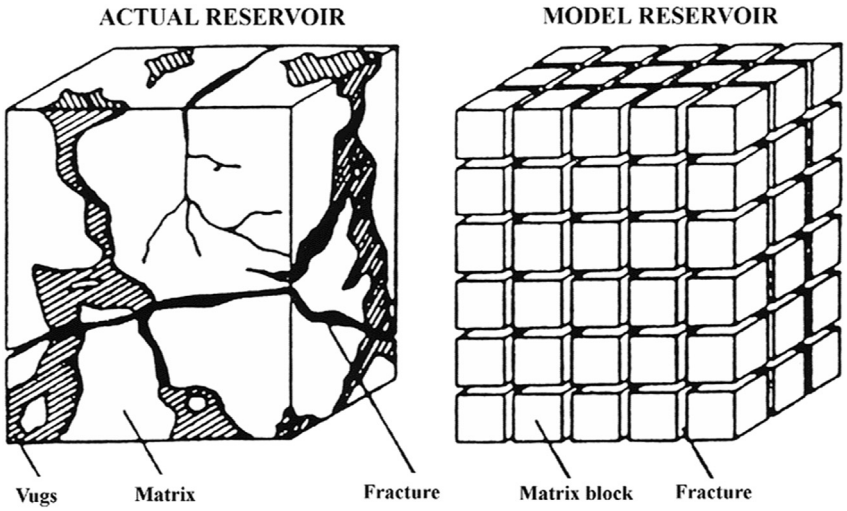

Fig. 1. Idealization of a fracture system (Warren and Root, 1963).

(<2 nm) and mesopores (2–50 nm). Storage in organic-rich shale has the advantage that the organic matter acts as molecular sieve, allowing CO_2, with linear molecular geometry, to accumulate in small pores where other naturally occurring gases such as methane (CH_4) cannot access. Additionally, the energy of molecular–interactions between the organics and CO_2 molecules is different, leading to a preferential and enhanced adsorption of CO_2 relative to CH_4. Thus the affinity of shale to CO_2 is partly due to steric and thermodynamic effects similar to those of coals that have been considered for enhanced coalbed-methane recovery (Kang et al., 2011).

As an unconventional reservoir, the porosity and permeability of shales are significantly lower than that of conventional reservoirs but have features that are similar to coalbed reservoirs (Shi and Durucan, 2010; Soeder, 2011; Wang et al., 2012). These features include matrix-dominated storage, fracture-dominated transport and sorption as a significant component of the overall gas budget. The significant sorption potential of gas shales makes them a viable medium for the sequestration of CO_2.

Naturally fractured reservoirs such as shales and coalbeds have been traditionally modeled using the dual porosity concept (Warren and Root, 1963). Gas is physically adsorbed to the surface of the porous shale structure and is transported by diffusion (Fig. 1). Fractures provide high permeability but low storage pathways to access the low permeability but high storage medium of the matrix. Gas desorbs from the pores and is transported by Fickian diffusion to the fractures where transport is by Darcy's law.

Prior work (Vermylen, 2011) has shown that gas adsorption in gas shale follows the monolayer adsorption-Langmuir isotherm (Vermylen, 2011). Langmuir isotherm parameters describe the relationship between TOC content, pressure, and the adsorbed gas-carrying capacity of the sorbing media (Lyster, 2012). Between 20% and 85% of total storage in shale may be in the form of adsorbed gas (Freeman et al., 2013), and the majority of this gas may never be produced due to the steepness of the sorption isotherm at lower pressure. Thus, injecting a higher affinity gas like CO_2 may be a feasible method to sweep for CH_4 and therefore enhance its recovery. The Langmuir volume constant can be estimated from a density log or TOC log. Total organic carbon (TOC) relates to the source material that generated the resulting gas or liquid hydrocarbon as well as the adsorption capacity of a shale to retain gas sorbed in the matrix. Studies show that adsorbed gas, free gas stored in the matrix, increases linearly with total organic content (Jarvie, 2004).

This study examines the behavior of a prototype reservoir swept by CO_2 to determine the feasibility of ESGR as a recovery technique. The lithotype used is the Barnett shale due to the availability of petrophysical data. The Barnett shale is an organic-rich, petroliferous black shale of middle–late Mississippian age with 4–8% organic carbon content (TOC), 20–40% illite clay, and no free water, long known as a probable source rock for hydrocarbons throughout north-central Texas (Montgomery et al., 2005; Goodway et al., 2006). Estimates for original gas in place for Barnett gas resource are in the order of 200 tcf, with ultimate technically recoverable reserves variably assessed within the range 3–40 tcf (Jarvie et al., 2003; Pollastro et al., 2003; Schmoker et al., 1996). The potential for ESGR by CO_2 is predicated on the observation that shale has a greater affinity of CO_2 over CH_4. In Barnett shale, at low pressures (600 psi), preferential adsorption of CO_2 over CH_4 ranges from 3.6x to 5.5x on a mass basis; at high pressure, this preferential adsorption of CO_2 over CH_4 may reach 5x to 10x (Vermylen, 2011). When CO_2 is injected into a depleted shale formation – even one that has previously been stimulated – the rock will release more methane because pockets of the gas chemically trapped within the shale will be released in favor of the more chemically sorptive CO_2. Two parameters are important regarding CO_2 storage in porous media. The first is whether sufficient capacity exists in the reservoir to store the intended volume of CO_2, which is controlled by the sorptive capacity. The second is whether sufficient injectivity exists and can be maintained to allow the penetration of CO_2 at the desired supply rate and deep into the reservoir.

Previous simulation work on Barnett shale shows that the time evolutions of gas pressure, stress-dependent permeability and porosity, and effective stresses are strongly influenced by gas desorption during production, especially near the wellbore (Huang and Ghassemi, 2011). Other simulation studies also show that CO_2 injection for enhanced gas recovery and concurrent CO_2 sequestration is technically and economically feasible but with principal obstacles related to the potential contamination of the production stream by CO_2 and high costs involved in the process (Khan et al., 2012). Simulation studies have been carried out to comprehend by which process CO_2 sequestration in a depleted gas reservoir might result in enhanced gas recovery. These have included the effect of mixing (CO_2–CH_4) on the recovery process prior to reservoir depletion (Khan et al., 2012) and were mainly directed to reduce greenhouse gas emissions in the atmosphere by sequestering in a depleted gas reservoir or in an aquifer (Benson, 2006; Clemens and Wit, 2002; Knox et al., 2002; Mamora and Seo,

2002; Oldenburg et al., 2001; Ozkilic and Gumrah, 2009). Previous study also showed that continuous CO_2 injection could be feasible for enhanced the gas recovery but huff-n- puff method might not be a good option (Schepers et al., 2009).

In this work we use a dual porosity model incorporating adsorptive behavior and with sorption/swelling dependent porosity and permeability to examine the potential for CO_2 as a stimulation medium for ESGR. In particular we examine the potential rates of injection and storage of CO_2 relative to rates of recovery of CH_4 to examine crucial issues of reduced injectivity and early breakthrough of CO_2. We examine this behavior for different CO_2 injection schedules including steady and pulsed injection to determine an optimal injection schedule which can maximally enhance CH_4 recovery but control CO_2 early breakthrough and minimize the cost of CO_2 injection and separation.

2. Model development

We develop a model for multi-component transport in dual porosity sorbing and swelling media. The following introduces key models describing porosity and permeability evolution in both matrix and fracture networks including the coupling between these two media.

2.1. Field and constitutive equation

Field and constitutive equations for gas flow and transport in shale are defined (Kumar et al., 2013b). These equations are coupled through porosity and permeability evolution driven by Langmuir sorption and swelling in the shale matrix with sympathetic influence on the deformation and permeability response of the fracture. The following assumptions apply:

1) The shale reservoir is a homogenous, isotropic and elastic continuum. The system is isothermal.
2) Gas present within the system is ideal and its viscosity is constant under isothermal conditions.
3) Gas flow through the fractures in shale conforms to Darcy's law (the water phase is not considered in this study); gas transport in the shale matrix is assumed to obey Fick's law.
4) Gas sorption only occurs within the matrix.

2.1.1. Binary gas adsorption

Barnett shale usually contains more than 80% CH_4 augmented by a mixture of other heavier hydrocarbons as well as CO_2 and N_2 (Bullin and Krouskop, 2008). In this study, it is assumed that the gas shale reservoir contains only two species: CH_4 (fracture: 95%; matrix: 87.5%) and CO_2 (fracture: 5%; matrix: 12.5%) as these two species exert the major control on transport in gas shale. The initial gas pressures of CH_4 and CO_2 in the reservoir are assumed to be 22.8 MPa and 1.2 MPa respectively in the fracture network and 1.143 MPa and 22.857 MPa respectively in the matrix. This constitutes an overall initial pressure in the reservoir of 24 MPa, representing reservoir pore pressure at a depth of 7000–8000 feet.

The gas adsorbed in the shale matrix follows Langmuir sorption behavior (Vermylen, 2011). The Langmuir adsorption isotherm assumes that the gas is present as a monolayer. The gas volume adsorbed per unit mass of shale can be calculated from the Langmuir isotherm (Langmuir, 1916) as

$$V = \frac{V_L p_m}{p_m + p_L} \tag{1}$$

where V_L is the Langmuir volume constant, representing the maximum volume of gas that can be adsorbed per unit mass of shale at infinite pressure, p_L is the Langmuir pressure, representing the pressure at which the Langmuir volume can be absorbed in the matrix, p_m is the equilibrium pressure of gas in the matrix and V is the volume adsorbed per unit mass of shale at pressure p_m.

The gas adsorbed in the shale is not always pure CH_4. Shale can also adsorb appreciable amounts of CO_2, N_2 and heavier hydrocarbons such as ethane and propane. Each gas does not "sorb" independently, but rather competes for the same sorption sites. The multi-component adsorption behavior may be expressed by the extended Langmuir isotherm (ELI) as

$$V_k = \frac{V_{k0} C_k b_k'}{1 + \sum_{j=1}^{N} C_j b_j'} \tag{2}$$

where V_{k0} is the adsorbed volume of species k per unit mass of shale at infinite pressure, C_k is the equilibrium concentration of gas in the matrix, b_k' is equal to RT/p_L and V_k represents the volume adsorbed per unit mass of shale at concentration c_m for species k. By analogy, the contribution of each gas species in an n-species mixture to the sorption-induced volumetric strain can be described as (Wu et al., 2011)

$$\varepsilon_k = \varepsilon_{Lk} \frac{C_k b_k'}{1 + \sum_{j=1}^{n} C_j b_j'} \tag{3}$$

Hence, the total sorption induced strain can be determined by summing the contributions from each individual gas species (Wu et al., 2011)

$$\varepsilon_s = \sum_{k=1}^{n} \varepsilon_k = \sum_{k=1}^{n} \varepsilon_{Lk} \frac{C_k b_k'}{1 + \sum_{j=1}^{n} C_j b_j'} \tag{4}$$

where ε_{Lk} is the Langmuir strain for species k, representing the strain caused by species k at infinite pressure, ε_k is the strain developed at concentration C_k in the matrix for gas k and ε_s is the total strain developed by the presence of the gas mixture.

2.1.2. Porosity model for matrix and fracture

Since shale and coal both follow the Langmuir isotherm, a constitutive model developed for the evolution of porosity in coal (Wu et al., 2011) is employed in this study to investigate the response of shale.

For sorption induced by a binary gas mixture, the matrix porosity can be expressed as

$$\varphi_m = \varphi_{m0} - \frac{\alpha}{K} \frac{1}{\frac{b_0}{a K_f} + \frac{1}{K}} \left(\sum_{k=1}^{2} \varepsilon_{Lk} \frac{C_{mk} b_k'}{1 + \sum_{j=1}^{n} C_{mj} b_j'} - \varepsilon_v \right) \tag{5}$$

where φ_m is the matrix porosity, φ_{m0} is the initial matrix porosity, α is the Biot coefficient for the shale matrix, K is the matrix bulk modulus, K_f is the modified fracture stiffness, which is equal to the product of initial fracture aperture and fracture stiffness, b_0 is the initial fracture aperture, a is the fracture spacing, ε_{Lk} the Langmuir strain for species k, C_{mk} is the equilibrium concentration of gas k in the matrix, b_k' is equal to RT/p_L for species k, and ε_v is the volumetric strain of the shale, which is considered zero in this study, since all four sides of the model geometry are assumed to be constrained.

Similarly, the porosity of the fracture can be expressed as

$$\frac{\varphi_f}{\varphi_{f0}} = 1 - \frac{3}{\varphi_{f0} + \frac{3K_f}{K}} \left(\sum_{k=1}^{2} \varepsilon_{Lk} \frac{C_{mk} b_k^{'}}{1 + \sum_{j=1}^{n} C_{mj} b_j^{'}} - \varepsilon_v \right) \tag{6}$$

where φ_f is the fracture porosity, φ_{f0} is the initial fracture porosity and the subscripts m and f refer to matrix and fracture respectively.

2.1.3. Permeability model for matrix and fracture

Similarly, the relations derived for coal can also be employed for the permeability evolution of the shale matrix (Wu et al., 2011),

$$\frac{k_m}{k_{m0}} = \left(1 - \frac{\alpha}{\varphi_{m0} K} \frac{1}{\frac{b_0}{aK_f} + \frac{1}{K}} \left(\sum_{k=1}^{2} \varepsilon_{Lk} \frac{C_{mk} b_k^{'}}{1 + \sum_{j=1}^{n} C_{mj} b_j^{'}} - \varepsilon_v \right) \right)^3 \tag{7}$$

where, k_m is the permeability of the matrix and k_{m0} is the initial matrix permeability.

To incorporate the effects of effective stress, sorption induced swelling and the occluding effect of moisture, the behavior of the fracture may be recast as (Kumar et al., 2012)

$$\frac{k_{fk}}{k_{f0k}} = \left\{ \left(1 + \frac{C_k p_{mk}}{p_{mk} + p_{Lk}} \right)^3 + e^{-\beta_k \sigma'} \right\} * e^{-\delta_k S_w} \tag{8}$$

where k_{fk} is the fracture permeability for species k, k_{f0k} is the initial permeability of species k in the fracture, p_{mk} is the gas pressure of species k in the matrix, p_{Lk} is the Langmuir pressure constant for species k, σ' is the effective stress, defined as equivalent to confining stress minus gas pressure, S_w is the moisture content of the shale, in this case, considered zero, δ_k is the fitting parameter for species k, representing the occluding effect of moisture, C_k is another fitting parameter for species k, representing the influence of effective stress, $C = \left(\frac{\varepsilon_L s^2}{a b_0} \right)$, where s is the fracture spacing, a is the fracture length, b_0 is the initial fracture aperture, ε_L is the peak Langmuir strain, and β_k is also a fitting parameter for species k, representing the effect of sorption induced swelling (Kumar et al., 2013a).

2.1.4. Matrix and fracture coupling

The matrix may act as both source or sink depending upon the pressure (or concentration) differential between matrix and fracture. The mass balance between fracture and matrix incorporates convective, diffusive, and transfer flux flow.

2.1.4.1. EOS for an ideal gas. The response of the matrix and fracture are coupled through the equation of state (EOS) for an ideal gas, which describes the relation between pressure, volume and temperature in both matrix and fractures

$$pV = nRT \tag{9}$$

where p [Pa] is the pressure, V [m^3] is the volume, R $\left[m^3 \cdot \frac{Pa}{K \cdot mol} \right]$ is the gas constant, n is the molar concentration and T [K] is the temperature. Similarly, the concentration C of the species may be represented as $C = n/V$ [units of mol/m^3] resulting in

$$p = CRT \tag{10}$$

allowing pressures to be uniquely linked to concentration.

2.1.4.2. Mass transfer between matrix and fracture. For a fracture network of orthogonal fractures of equal fracture spacing, matrix and fracture can also be coupled through a transfer flux ω_k between these two media for a component of gas k (Mora and Wattenbarger, 2009) as

$$\omega_k = -\frac{3\Pi^2}{a^2} \tag{11}$$

where ω_k is the shape factor, controlling drainage rate from matrix to the fracture. In a unit volume of fracture, the mass of the species and its mass rate of change is the net result of advection of the species into or out of this volume which is governed by Darcy flow $\nabla \cdot \left(-\frac{k_f}{\mu} p_f \nabla \cdot p_f \right)$ and gain or loss of the species from this volume due to exchange with the matrix $\pm \frac{3\Pi^2}{a^2} \frac{k_m}{\mu} p_f (p_f - p_m)$ (Kumar et al., 2013b)

3. Model implementation

This model follows the transport of binary species in a fractured porous reservoir pierced by parallel horizontal wells. The horizontal well pattern includes a production well located at the center of a rectangular section that cuts the reservoir vertically and is flanked by twin injection wells as shown in Fig. 2. The reservoir has been artificially fractured to elevate the permeability of the stimulated reservoir volume – taken as the full reservoir shown in Fig. 2.

Symmetry of the injection-withdrawal system allows a one-quarter section of the full-field reservoir to represent the full system (see red dashed line (in the web version)). This one-quarter section of the reservoir is represented by a 2D block with sides 120 m × 60 m (Fig. 3). The diameter of the wells is assumed to be 0.0762 m (3 inches), a typical value for wellbores. The model has no flow-no flux condition on all four sides except the wellbores. Production volumes are evaluated by multiplying production from this 1 m section by the total presumed well length. The initial gas pressure in the reservoir is 24 MPa, representing the pore pressure at a depth of 7000–8000 ft. The initial pressures of CH_4 and CO_2 are set according to their composition. CH_4 has an initial pressure of 22.8 MPa in fracture and 22.857 MPa in the matrix, based on partial pressures. For CO_2, the values are 1.2 MPa and 1.143 MPa, respectively. The production well produces at a bottomhole pressure of 0.1 MPa. Different injection rates and schedules, including continuous injection and pulsed injection are used. The injection rate is controlled by setting the injection wellbore pressure differently as (i) no injection (sealed boundary); (ii) 0 MPa overpressure (same

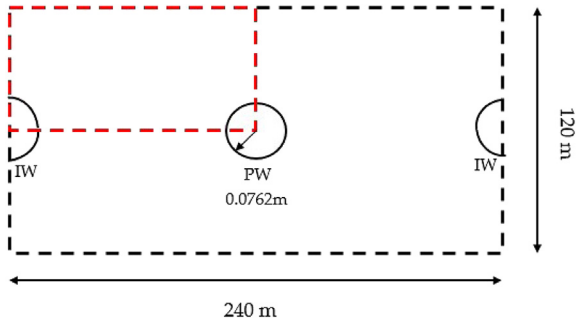

Fig. 2. Horizontal wells pattern with one production well (PW) at the center flanked by injection wells on each side (IW) and representing a repeating array of injectors and recovery wells.

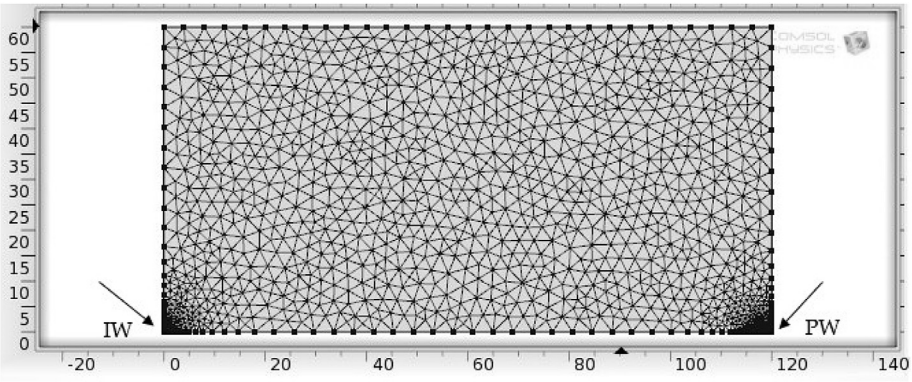

Fig. 3. Schematic of a one-quarter section of the longitudinal section of the entire reservoir with horizontal wells.

Table 1
Modeling parameters used in simulations.

Symbol	Parameter	Value	Unit
E	Young's Modulus of shale	32.75 (Goodway et al., 2006)	*GPa*
E_S	Young's Modulus of shale grain	40.54 (Vermylen, 2011)	*GPa*
N	Poisson's ratio of shale	0.235 (Goodway et al., 2006)	–
ρ_s	Density of shale	2.5×10^3 (Kuuskraa et al., 1998)	kg/m^3
μ_{CH_4}	CH_4 dynamic viscosity	1.15×10^{-5} (Wu et al., 2011)	$Pa{\cdot}s$
μ_{CO_2}	CO_2 dynamic viscosity	1.60×10^{-5} (Wu et al., 2011)	$Pa{\cdot}s$
P_{L,CH_4}	CH_4 Langmuir pressure constant	11 (Vermylen, 2011)	*MPa*
P_{L,CO_2}	CO_2 Langmuir pressure constant	8.64 (Vermylen, 2011)	*MPa*
V_{L,CH_4}	CH_4 Langmuir volume constant	1.05×10^{-3} (Vermylen, 2011)	m^3/kg
V_{L,CO_2}	CO_2 Langmuir volume constant	4.93×10^{-3} (Vermylen, 2011)	m^3/kg
ε_{L,CH_4}	CH_4 Langmuir volumetric strain constant	8.1×10^{-4}	–
ε_{L,CO_2}	CO_2 Langmuir volumetric strain constant	3.6×10^{-3} (Vermylen, 2011)	–
$\varnothing_{m_0}$	Initial porosity of matrix	0.041 (Strickland et al., 2011)	–
$\varnothing_{f_0}$	Initial porosity of fracture	0.007 (Reed and Wang, 2009)	–
k_{m_0}	Initial permeability of matrix	2.17×10^{-19} (Strickland et al., 2011)	m^2
k_{f_0}	Initial permeability of fracture	2.27×10^{-17} (Strickland et al., 2011)	m^2
a	Fracture spacing	0.025	*m*
b_0	Initial fracture aperture	5×10^{-4}	*m*

pressure as the initial reservoir pressure); (iii) 4 MPa overpressure (4 MPa higher than the initial reservoir pressure), and (iv) 8 MPa overpressure (8 MPa higher than the initial reservoir pressure).

Appropriate input variables are as shown in Table 1. Each simulation is run for 10^9 seconds (~ 30 years).

4. Results and discussion

Models of continuous and pulsed injection are explored to investigate the evolution of permeability and the production of CH_4 and CO_2 together with the potential for early breakthrough. The desire is to define an optimal injection schedule with no or mitigated CO_2 early breakthrough, minimum cost of CO_2 injection as well as to determine the level of enhanced CH_4 production.

4.1. Continuous injection

Four injection cases are explored that represent no injection, 0 MPa overpressure injection, 4 MPa overpressure injection and 8 MPa overpressure injection. The evolution of permeability and concentration in matrix and fracture, CH_4 production, CO_2 early breakthrough as well as the CO_2 sequestration capacity of the reservoir are investigated.

4.1.1. Permeability evolution in matrix and fracture

As gas desorbs from the shale, the matrix shrinks and the fracture widens, although this may be offset by a reduction of fracture aperture because of increased net stress caused by reservoir-pressure depletion. In addition, the adsorption of CO_2 and related swelling in the shale matrix causes permeability to decrease. Permeability is controlled by pore volume compressibility (in the early time) and matrix swelling/shrinkage (in late time). During the first ~ 100 days, the matrix permeability remains near constant for all continuous injection cases including the no injection case since this period is dominated by fracture flow (Fig. 4). Gas production comes mainly from the fracture during this early time as the fracture is a preferred flow conduit. After ~ 100 days, when the free gas in the fracture has been largely depleted, the matrix flow begins to contribute. After ~ 100 days, matrix permeability decreases with time by a factor of 0.9% ~ 1.3% indicating that it is in the effective-stress-effect regime when the pressure in matrix decreases. Permeability loss is also controlled by fracture geometry, Langmuir swelling coefficient and void “stiffness”, whereas the rate of permeability increase is controlled by fracture geometry and void “stiffness”. For the higher injection pressure case (8 MPa overpressure injection), the decrease of matrix permeability is not as significant as for the lower injection pressure case (0 MPa overpressure injection) in that the pressure decrease, to an extent, is compensated for by the injection.

The fracture permeability is increased by ~ 1/3 in the three injection cases as fractures dilate as the gas pressure increases, whereas for the no injection case, it increases only by a factor of 1.8% - higher injection pressures result in more significant dilation

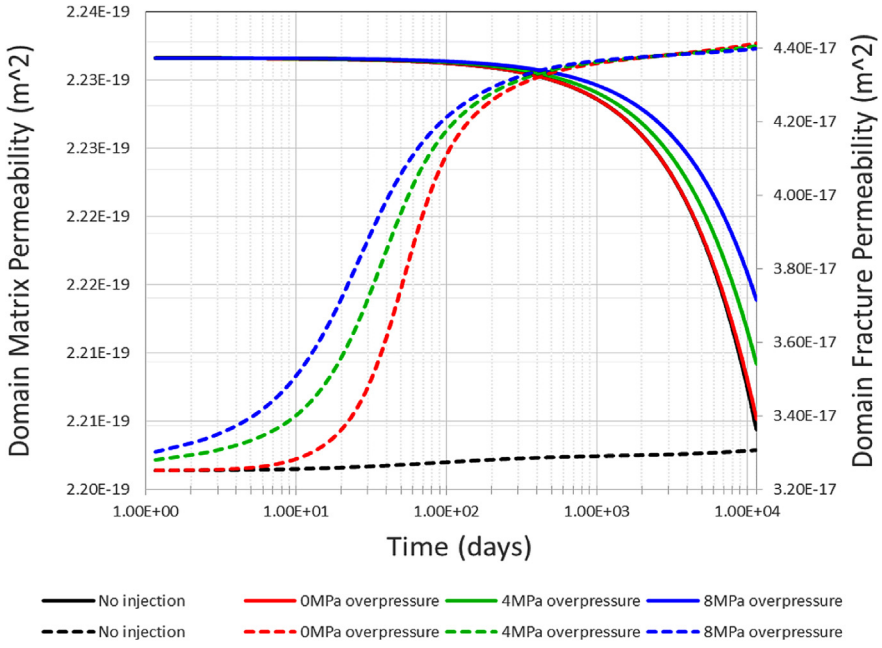

Fig. 4. The average permeability of the matrix (solid lines) and fracture (dashed lines) under continuous injection.

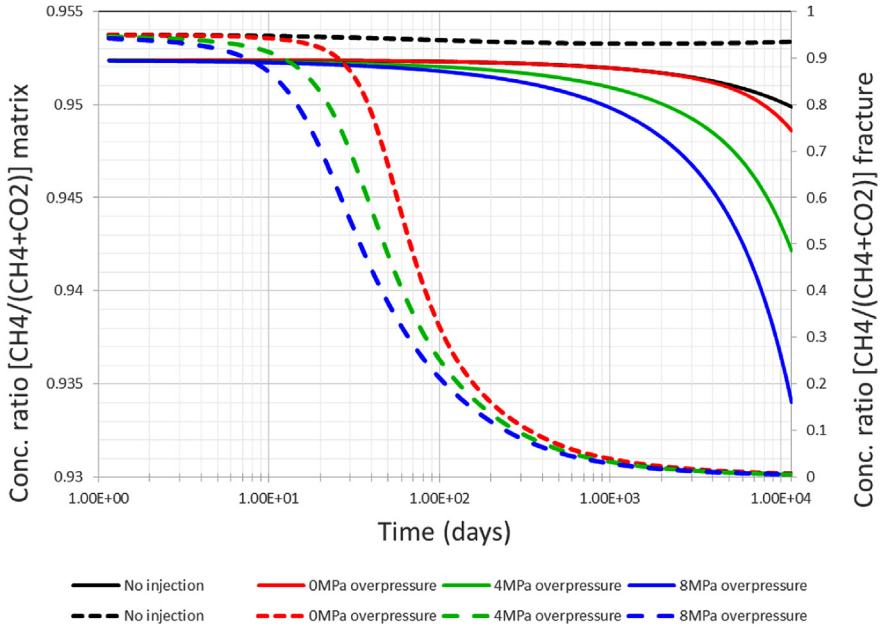

Fig. 5. The evolution of the ratio of average concentration of $CH_4/(CH_4 + CO_2)$ in the matrix (solid lines) and fracture (dashed lines) under continuous injection.

hence increases in permeability. Therefore higher CO_2-injectivity results in higher gas production, solely due to the mechanical effect.

4.1.2. Concentration evolution in matrix and fracture

The recovery of CH_4 relative to the invasion of CO_2 may be represented by the ratio, $CH_4/(CH_4 + CO_2)$ where a small ratio represents effective recovery of methane. The evolution of this ratio $CH_4/(CH_4 + CO_2)$ in matrix and fracture, again, demonstrates there two stages exist: fracture dominant flow and matrix dominant flow (see Fig. 5). The decrease of CH_4 concentration occurs almost immediately in the fracture following the injection of CO_2. Then only after ~100 days, the decrease of CH_4 concentration in the matrix became significant. Conversely, the concentration ratio in the fracture remains stable, indicating that within the first 100 days, CH_4 production comes mainly from the fracture which provides a preferred conduit; then after 100 days, when the free gas in the fracture is exhausted, CH_4 production mainly comes from the matrix, since CO_2, with a higher adsorption affinity, competes with CH_4 for the adsorption sites in the matrix and sweeps out the CH_4. Observed from these three cases with CO_2 injection is that higher injection pressure contributes to faster and more significant $CH_4/(CH_4 + CO_2)$ concentration drop because of the faster and more efficient sweep by the front of CO_2.

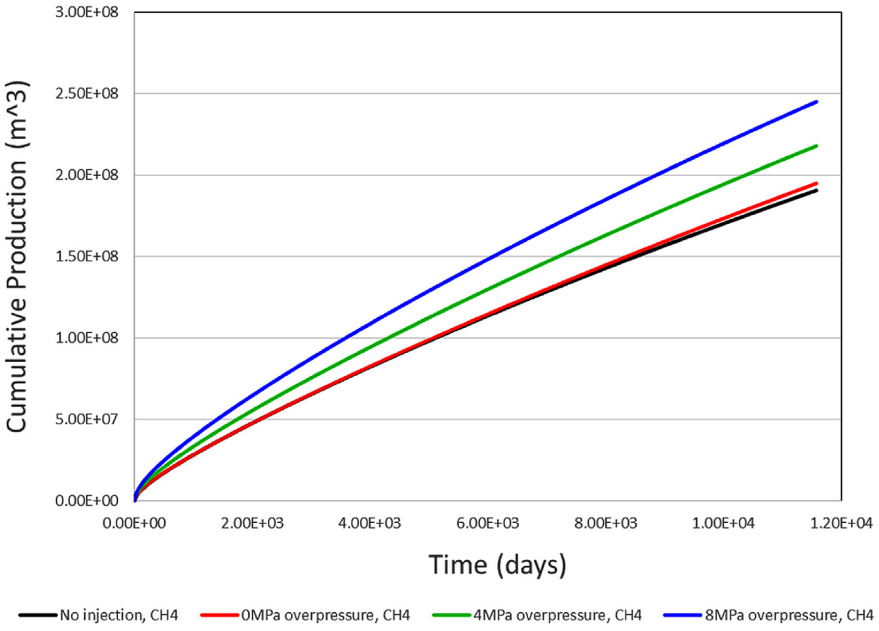

Fig. 6. CH_4 cumulative production under continuous injection.

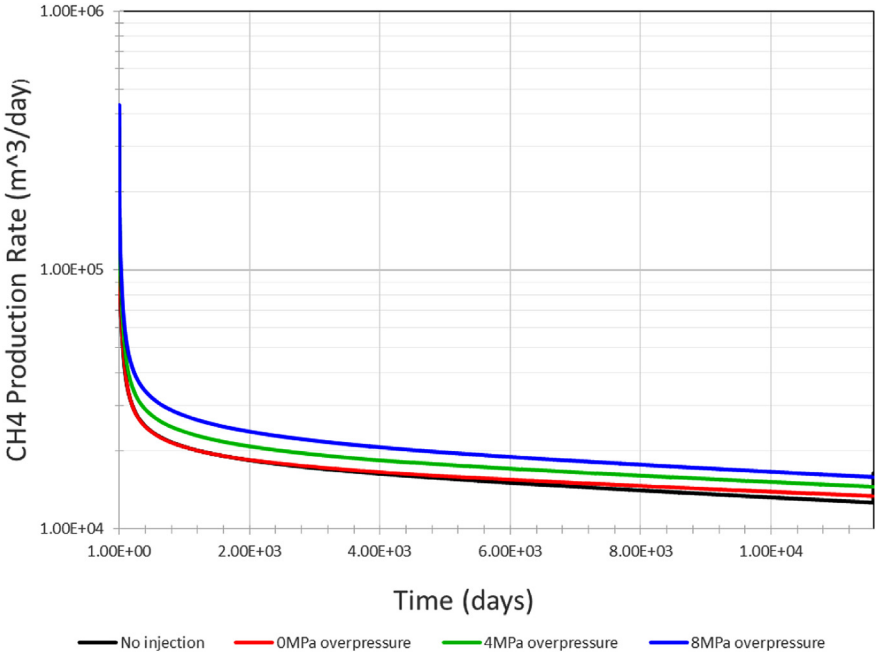

Fig. 7. CH_4 instantaneous production rate under continuous injection.

4.1.3. CH_4 gas production

The cumulative production of CH_4 over 30 years is shown in Fig. 6. The elevation of CH_4 gas production is 2.26%, 14.26%, and 28.5% for 0 MPa, 4 MPa and 8 MPa overpressure injection, respectively. It is clear that the highest injection pressure, with the highest injectivity and elevated permeability, still results in the maximum production of CH_4.

The recovered gas rate depends on 1) the ratio of relative volume of organic matter to total porosity, permeability, geometry, distribution, and connectivity of organic flakes; 2) how organic matter is connected to natural and hydraulic fractures; and also, in this study, 3) the injectivity of CO_2. The instantaneous production of CH_4 (Fig. 7) shows these two flow regimes mentioned above—fracture dominant flow and matrix dominant flow. The former, a rapid process, is affected by fracture permeability and reservoir length. The latter, a slower rate-inhibited process, is influenced by matrix hydraulic conductivity and matrix block length.

4.1.4. CO_2 early breakthrough

Understanding mechanisms involved in the early breakthrough of CO_2 is one of the foci of CO_2-ESGR projects in that separation of CO_2 from CH_4 is costly. Another reason for minimizing the early breakthrough of CO_2 is consideration of environmental security — with the desire for the entire system to be near net neutral in terms

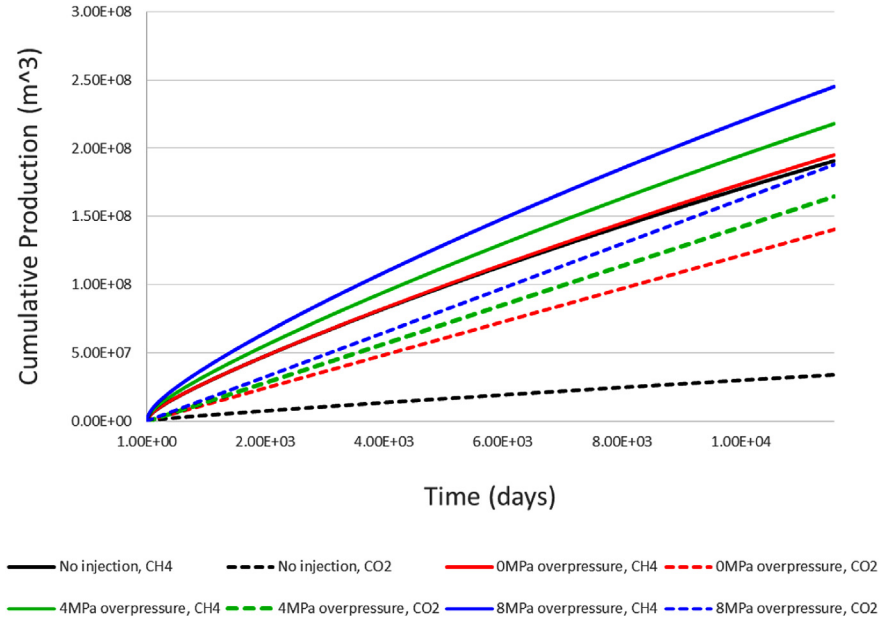

Fig. 8. Cumulative production of CH_4 (solid lines) and CO_2 (dashed lines) under continuous injection.

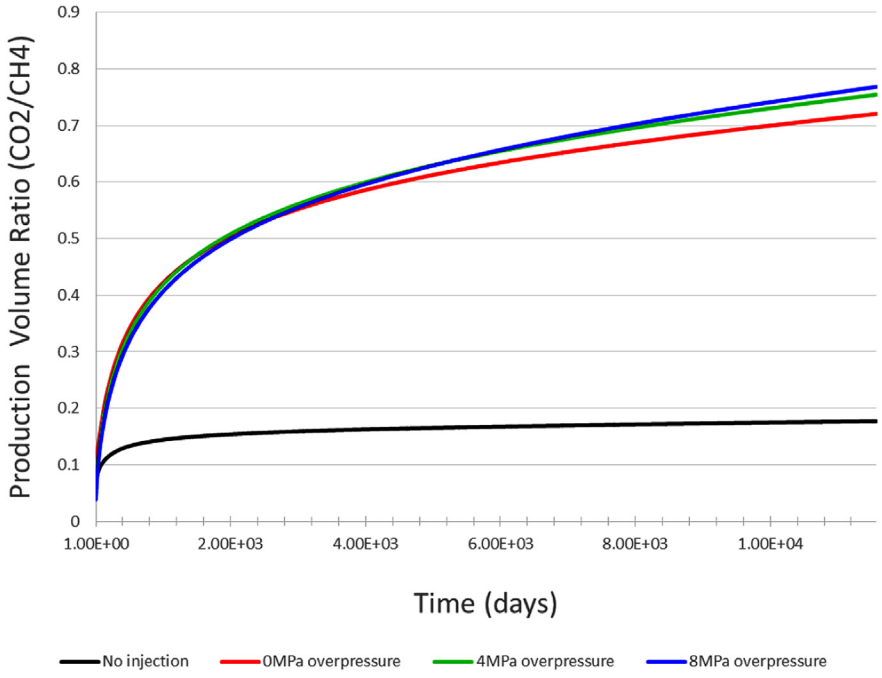

Fig. 9. Volume ratio of CO_2/CH_4 at the production well under continuous injection.

of carbon footprint with corresponding positive impact on induced seismicity. Conversely, reservoir re-pressurization, a process when CO_2 is re-injected into the reservoir at a high rate to re-pressurize the reservoir has the benefit of both preventing subsidence/stress-change after the reservoir is depleted and of increasing incremental gas recovery. Thus one of the goals of this study is to determine the optimum CO_2 injection schedule to yield maximum CH_4 gas production as well as alleviating early CO_2 breakthrough. CO_2 breakthrough, in this paper, is defined as the volume ratio of CO_2/CH_4 at the production well higher than the value for the no injection case. Figs. 8 and 9 indicate that CO_2 breakthrough is presents in all three injection cases. The volume ratio of CO_2/CH_4 at the production well for these three cases are 0.72, 0.75, and 0.77, respectively. CO_2 breakthrough occurs as soon as the matrix-dominant flow regime begins, indicating that a considerable mass of CO_2 transits to the production well directly through the preferred fracture channel. This undesirable effect may potentially be mitigated by pulsed CO_2 injection, by controlling the injection and shut in time span. This may mitigate early CO_2 breakthrough since CO_2 can be adsorbed during the shut-in period.

4.1.5. CO_2 sequestration

CO_2 sequestration is considered as another benefit of CO_2-ESGR. A fraction of the injected CO_2 can be stored in the reservoir, mainly

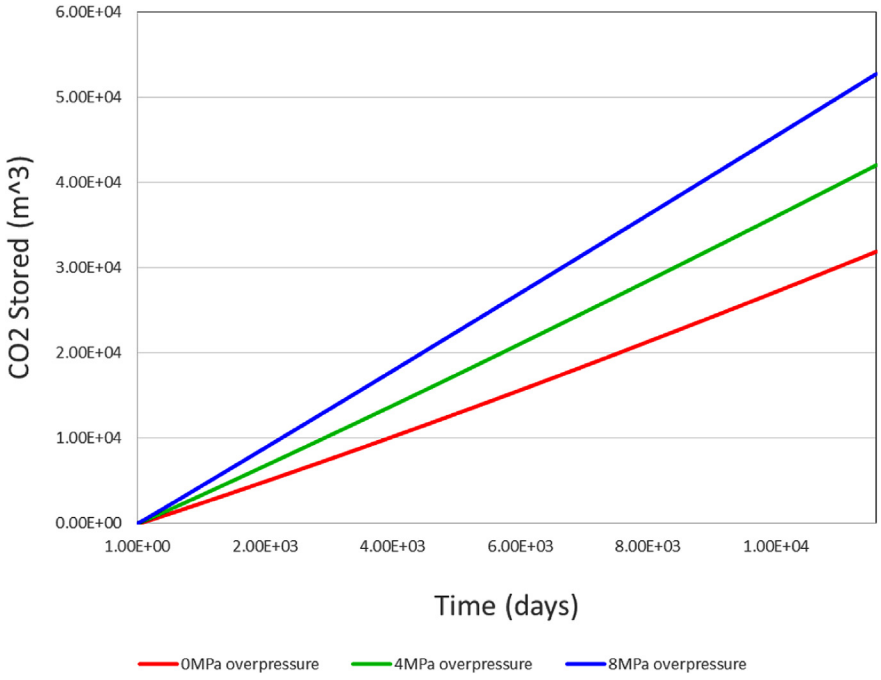

Fig. 10. CO_2 storage capacity under continuous injection.

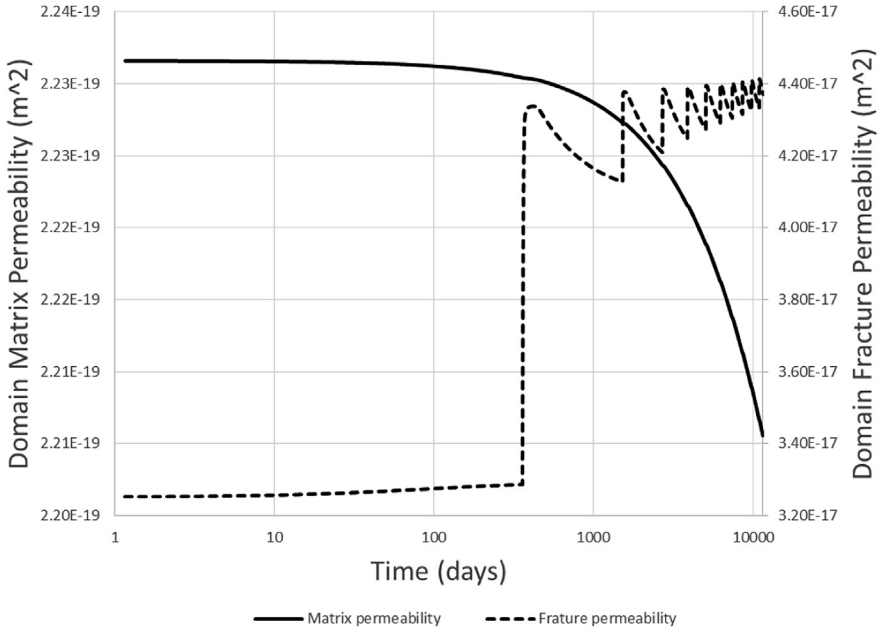

Fig. 11. The average matrix (solid line) and fracture (dashed line) permeability for optimal pulsed injection.

in the matrix in the form of adsorbed gas due to its high adsorptive affinity. CO_2 will be sequestrated in the reservoir in a supercritical state under higher pressure and temperature reservoir condition ($p > 7$ MPa and $T > 32$C). Fig. 10 shows that the CO_2 storage capacity is of the order of 10^4 m^3 when supercritical for the three injection cases. It is clear that the amount of CO_2 adsorbed is directly proportional to the injection pressure.

4.2. Pulsed injection

Although continuous injection results in significantly enhanced production, the severe breakthrough of CO_2 may be an issue due to the high expense of separation of CO_2 from CH_4. Multiple pulsed injection cases were performed to investigate the feasibility of this method. Here we present the results for the optimal pulsed injection case with maximum elevated CH_4 production with the requirement of no CO_2 early breakthrough for the reservoir parameters previously used. The gas shale reservoir is produced with no injection for 1 year, followed by CO_2 injection at an overpressure of 8 MPa for 3 months then shut in for 3 years repeatedly throughout the 30 year production life of the reservoir.

4.2.1. Permeability evolution in matrix and fracture

Permeability evolution under pulsed injection (Fig. 11) shows the same general trend as the continuous injection cases, namely, matrix permeability decreases and fracture permeability increases.

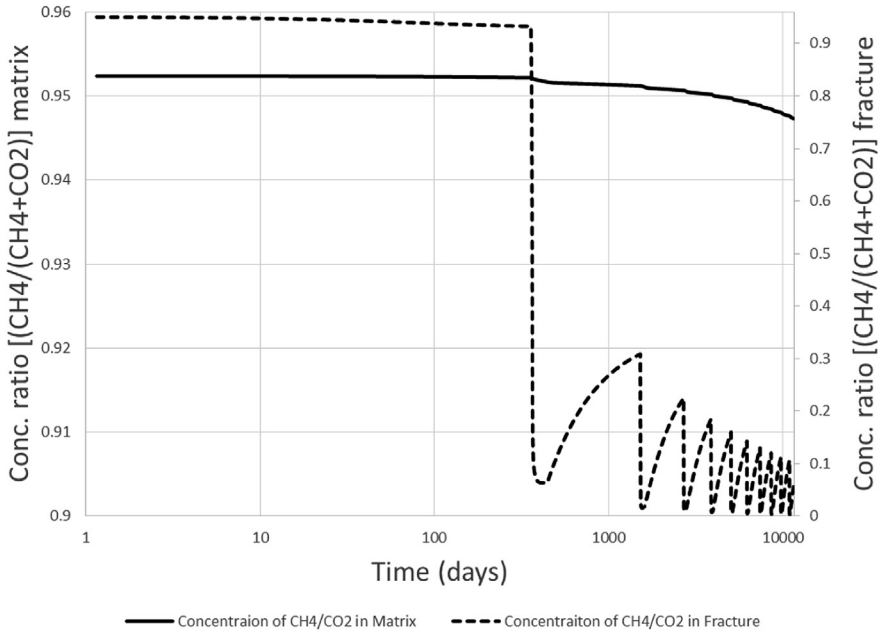

Fig. 12. The evolution of the ratio of average concentration of $CH_4/(CH_4 + CO_2)$ in the matrix (solid line) and fracture (dashed line) under optimal pulsed injection.

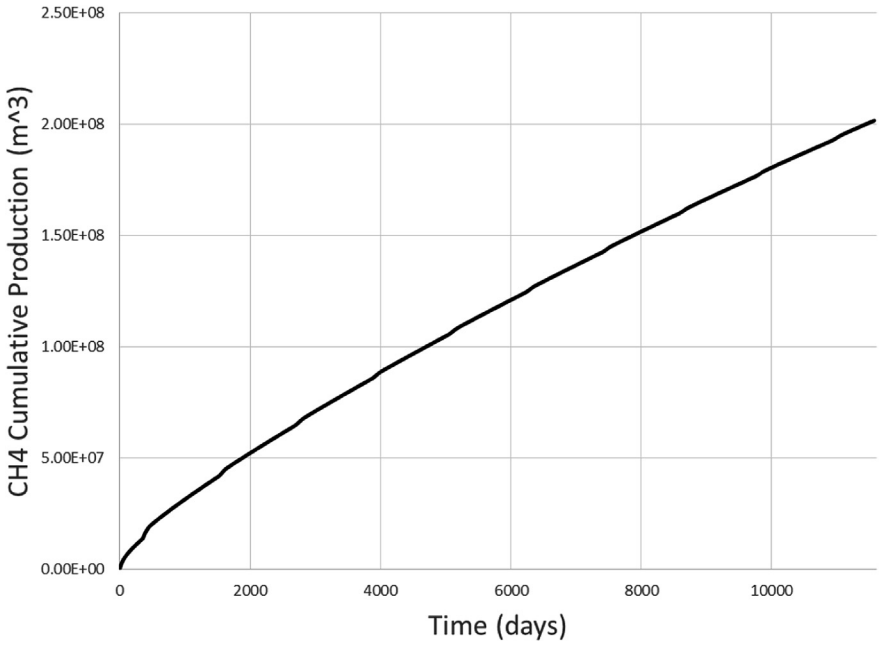

Fig. 13. CH_4 cumulative production under optimal pulsed injection.

The permeability of the fracture increases linearly with pressure by ~1/3, possibly because it reaches the Langmuir strain, the same magnitude as the continuous injection cases at the end of 30 years even though the total duration of injection is only 1.5 years. The extent of the decrease of matrix permeability is 1.3%, similar to the no injection case.

4.2.2. Concentration evolution in matrix and fracture

As soon as the injection starts (the first injection is at the end of the 1st year and lasts for 3 months), the concentration of CO_2 in the fracture increases rapidly since the fracture is a preferred flow channel. At the same time, a small drop in this concentration ratio is also observed in the matrix, indicating that CO_2 sweeps CH_4 from the reservoir by preferential absorption (Fig. 12).

4.2.3. CH_4 gas production

This optimal pulsed injection schedule can enhance CH_4 gas production by 9.34% (Fig. 13) compared with the no injection case. This occurs for a summed duration of CO_2 injection over the 30 year lifespan of the reservoir of only 1.5 years. Compared to the continuous injection case with an 8 MPa overpressure, this pulsed injection schedule can achieve 1/3 of the enhanced gas recovery at only 1/20 of the injection cost and absent CO_2 separation costs (no early breakthrough).

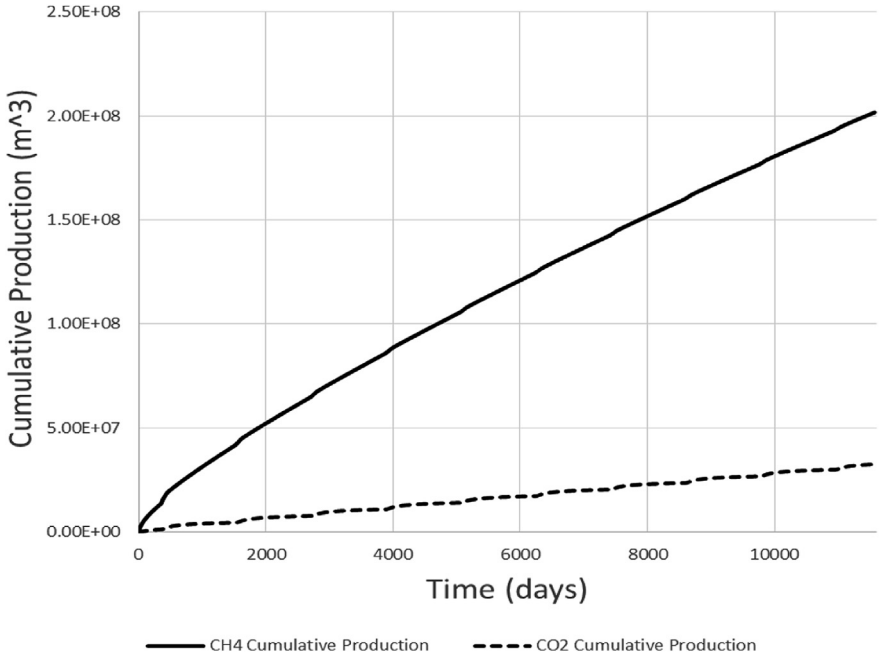

Fig. 14. Cumulative production of CH_4 (solid line) and CO_2 (dash line) under optimal pulsed injection.

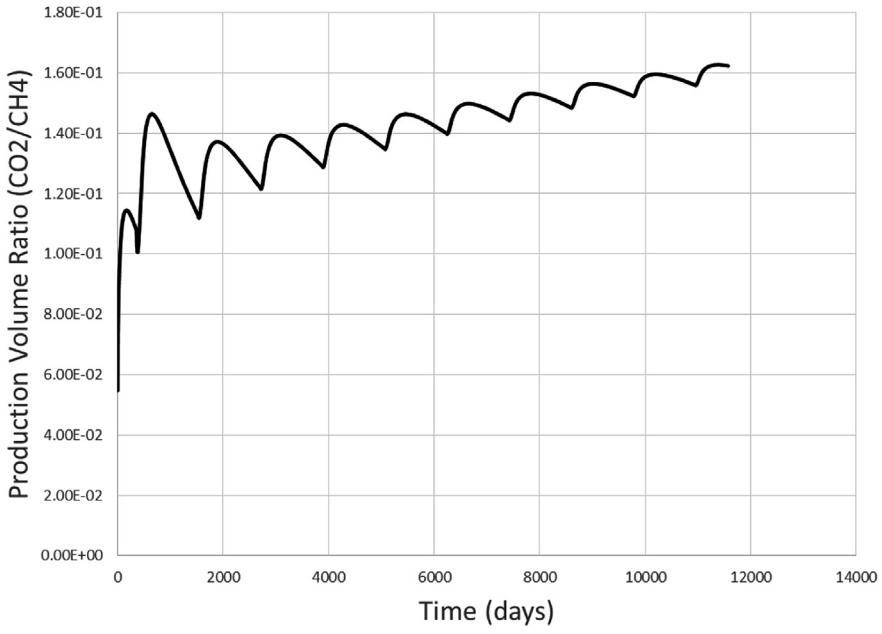

Fig. 15. Volume ratio of CO_2/CH_4 at the production well under optimal pulsed injection.

4.2.4. CO_2 early breakthrough

The principal incentive for pulsed injection is to mitigate early breakthrough of CO_2 - the volume ratio of CO_2/CH_4 at the production well must remain below the ratio for the no injection case (which is 0.18). For the pulsed injection case examined, there is no severe early breakthrough of CO_2 (Figs. 14 and 15), indicating that this schedule provides a feasible pathway for CO_2-ESGR with the benefit of enhanced gas recovery, at minimum cost of CO_2 injection as well as absent costs of CO_2 separation.

4.2.5. CO_2 sequestration

The storage capacity of the reservoir for injected CO_2 is shown in Fig. 16. The sequestration capacity reaches 6×10^3 m^3 under the selected pulsed injection schedule. Therefore storing CO_2 by adsorption in supercritical state within the matrix defines another intrinsic benefit of this pulsed injection schedule.

5. Conclusion

The applicability of enhanced CO_2-ESGR recovery in Barnett Shale is explored in this study. A dual porosity dual permeability model is used to describe the characteristics of the reservoir. A model of permeability evolution for sorbing dual porosity media originally developed for coal is applied to define response. Darcy's Law is used to describe flow within the fracture system with Fick's law applied to the matrix. Binary Langmuir adsorption theory is

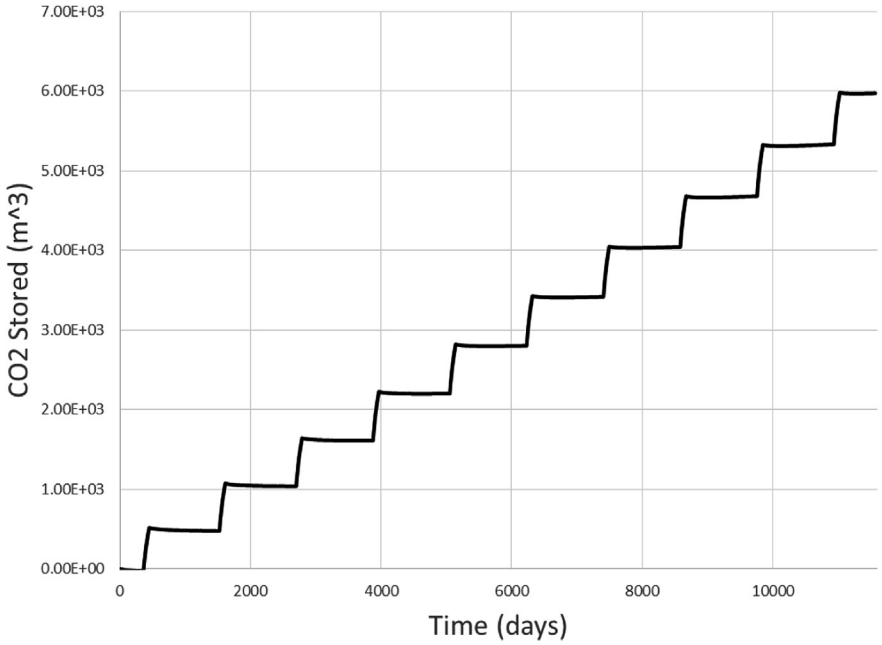

Fig. 16. CO_2 storage capacity under optimal pulsed injection.

adopted to represent the competitive adsorption between CO_2 and CH_4. Two forms of injection schedule are explored, representing continuous injection and pulsed injection. Both are compared with the no injection case as control to investigate the efficiency on enhanced gas recovery, CO_2 early breakthrough and CO_2 sequestration. The observations and conclusions are as follows:

1) Continuous CO_2 injection at overpressures of 0 MPa, 4 MPa, and 8 MPa enhance gas recovery by 2.26%, 14.26%, 28.5%, respectively. The net recovery of CH_4 over the lifetime of the reservoir is of the order of 10^8 m^3. However, at the same time, severe breakthrough of CO_2 occurs. At the end of the production life of the reservoir, the concentration of CH_4/CO_2 at the production wellbore for the three continuous injection cases is 0.72, 0.75, 0.77, whereas without injection this ratio is 0.18. Two distinct fluid flow stages are observed. These are for fracture dominated flow (within approximately the first 100 days of production) followed by matrix dominated flow (follows pressure breakthrough followed by mass depletion in the fracture system). Matrix permeability remains constant during the period of fracture dominated flow and decreases by only ~1% during matrix dominated flow; fracture permeability increases significantly during the first stage of fracture flow and is mildly elevated during the second stage of matrix dominated flow. Overall fracture permeability increases by ~1/3 for the injection scenarios followed, due to the dominant influence of CH_4 desorption relative to CO_2 sorption.
2) An optimal pulsed injection schedule with the total cumulative duration of injection of only 1.5 years (in 30 year reservoir life) elevates gas production by 9.24% compared to the no injection case. This increased productivity occurs with no early breakthrough of CO_2 together with a concomitantly reduced cost of CO_2 injection. Permeability evolution for this case shows the same trend as for continuous injection - the overall matrix permeability decreases by ~1% and the fracture permeability increases by ~1/3. Compared to the case for continuous injection at an overpressure of 8 MPa, this pulsed injection schedule achieves ~1/3 of the enhanced gas recovery for only 1/20 of the mass of CO_2 injected.
3) CO_2 is sequestrated in a supercritical status and is of the order of 10^4 m^3 for the continuous injection cases and 10^3 m^3 for pulsed injection case – representing only 10^{-4} to 10^{-5} of the mass of CH_4 recovered.

References

Benson, S.M., 2006. Monitoring carbon dioxide sequestration in deep geological formation for inventory verification and carbon credit. SPE Pap., 102833.
Bullin, K., Krouskop, P., 2008. Composition Variety Complicates Processing Plans for US Shale Gas. Annual Forum, Gas Processors Association.
Clemens, T., Wit, K., 2002. CO_2 enhanced gas recovery studies for an example gas reservoir. SPE Pap., 77348.
Freeman, C.M., Moridis, G., Ilk, D., Blasingame, T.A., 2013. A numerical study of performance for tight gas and shale gas reservoir systems. J. Pet. Sci. Eng., 22–39.
Goodway, B., Varsek, J., Abaco, C., 2006. Practical applications of P-wave AVO for unconventional gas resource plays – I: seismic petrophysics and isotropic AVO. CSEG Rec., 90–95. Special Edition.
Huang, J., Ghassemi, A., 2011. Poroelastic Analysis of Gas Production from Shale. ARMA, American Rock Mechanics Association, pp. 11–479.
Hussen, C., Amin, R., Madden, G., Evans, B., 2012. Reservoir simulation for enhanced gas recovery: an economic evaluation. J. Nat. Gas Sci. Eng., 42–50.
Jarvie, D., 2004. Evaluation of Hydrocarbon Generation and Storage in Barnett Shale, Fort Worth Basin, Texas. The University of Texas at Austin, Bureau of Economic Geology/PTTC, p. 116.
Jarvie, D.M., et al., 2003. Evaluation of Unconventional Natural Gas Prospects: the Barnett Shale Fractured Shale Gas Model. Poster presented at the 21st International Meeting on Organic Geochemistry. International Meeting on Organic Geochemistry, pp. 8–12.
Jenkins, C.D., MacNaughton, DeGolyer, Boyer, C.M., 2008. Coalbed- and shale-gas reservoirs. J. Pet. Technol., 92.
Kang, S.M., et al., 2011. Carbon dioxide storage capacity of organic-rich shales. SPE J., 842–855.
Khan, C., Amin, R., Madden, G., 2012. Economic modelling of CO_2 injection for enhanced gas recovery and storage: a reservoir simulation study of operational parameters. Energy Environ. Res., 65–82.
Knox, P.R., Hovorka, S.D., Oldenburg, C.M., 2002. Potential New Uses for Old Gas Fields: Sequestration of Carbon Dioxide. Gulf Coast Association of Geological Societies Transactions, pp. 563–571.
Kumar, H., et al., 2012. Optimizing enhanced coalbed methane recovery for unhindered production and CO_2 injectivity. Int. J. Greenh. Gases, 43 pp.
Kumar, H., Elsworth, D., Mathews, J.P., Marone, C., 2013a. Permeability Evolution Analogies in Sorbing Media: a Comparison Between Organic Shale and Coal (submitted for publication).
Kumar, H., Elsworth, D., Pone, D.J., Mathews, J.D., 2013b. Effect of CO_2 Injection on Homogeneously and Hetergenously Permeable Coalbed Reservoirs (submitted for publication).

Kuuskraa, V., Koperna, G., Schmoker, J., Quinn, J., 1998. Barnett shale rising Star in Fort Worth Basin. Oil Gas. J. 96 (21), 67.
Langmuir, I., 1916. The constitution and fundamental properties of solids and liquids part I solids. J. Am. Chem. Soc. pp. 38, 2221–2295.
Lyster, S., 2012. Quantification of uncertainty in shale gas resource estimates. GeoConvention.
Mamora, D., Seo, G., 2002. Enhanced Gas recovery by carbon dioxide sequestration in depleted gas reservoir. SPE Pap., 77347.
Montgomery, Scott L., Jarvie, Daniel M., Bowker, Kent A., . Pollastro, Richard M., 2005. Mississippian Barnett shale, Fort Worth basin, North-Central Texas: gas-shale play with multi–trillion cubic foot potential. AAPG Bull., 155–175.
Mora, C.A., Wattenbarger, R.A., 2009. Analysis and verification of dual porosity and CBM shape factor. J. Can. Pet. Technol., 17–21.
Oldenburg, C., Pruess, K., Benson, S., 2001. Process modelling of CO_2 injection into natural gas reservoirs for carbon sequestration and enhanced gas recovery. Energy Fuels, 293–298.
Ozkilic, O., Gumrah, F., 2009. Simulating CO_2 sequestration in a depleted gas reservoir. Energy Sources, Part A, 31, 13.
Pollastro, R.M., et al., 2003. Assessment of Undiscovered Oil and Gas Resources of the Bendarch–Fort Worth Basin Province of North-Central Texas and Southwestern Oklahoma. U.S. Geological Survey Fact Sheet 2004-3022, p. 2.
Reed, R.M., Wang, F.P., 2009. Pore networks and fluid flow in gas shale. SPE-124253-MS. Annual Technical Conference and Exhibition.
Schepers, K.C., Nuttall, B., Oudinot, A.Y., Gonzalez, R., 2009. Reservoir modeling and simulation of the Devonian gas shale of Eastern Kentucky for enhanced gas recovery and CO_2 storage. SPE, 126620.
Schmoker, J.W., et al., 1996. Production characteristics and resources assessments of the Barnett shale continuous (unconventional) gas accumulation, Fort Worth Basin, Texas: U.S. Geological Survey Open-file Report, p. 20.
Shi, J.Q., Durucan, S., 2010. Exponential growth in San Juan Basin Fruitland coalbed permeability with reservoir drawdown: model match and new insights. SPE Reserv. Eval. Eng., 914–925.
Soeder, D., 2011. Petrophysical Characterization of the Marcellus & Other Gas Shales. AAPG Eastern Section Meeting.
Strickland, R., Purvis, D., Blasingame, T., 2011. Practical Aspects of Reserve Determinations for Shale Gas. North American Unconventional Gas Conference and Exhibition.
Vermylen, J.P., 2011. Geomechanical Studies of the Barnett, Texas, USA. A Dissertation Submitted to The Department of Geophysics and The Committe on Graduate Studies of Standford University in Partial Fulfillment of The Requirments for The Degree of Doctor of Philosophy.
Wang, S., Elsworth, D., Liu, J., 2012. A mechanistic model for permeability evolution in fractured. J. Geophys. Res. 117 (B06205).
Warren, J.E., Root, P.J., 1963. The behavior of naturally fractured reservoirs. SPE J., 245–255.
Wu, Y., et al., 2011. A dual poroelastic model for CO_2-enhanced coalbed methane recovery. Int. J. Coal Geol. 86 (2–3), 177–189.